COMPRESSIVE RHEOLOGY : AN OVERVIEW

Ross G. de Kretser, David V. Boger and Peter J. Scales

Particulate Fluids Processing Centre, Department of Chemical Engineering
The University of Melbourne, Victoria 3010, Australia

ABSTRACT

Compressive rheology, or the behaviour of suspensions in sedimentation and compression has been widely studied and many theories, using different physical quantities, have evolved in parallel. This review article provides a basis for the reconciliation of these approaches via presentation of the Buscall-White (1987) approach to consolidation, which uses a compressive yield stress, $P_y(\phi)$, and a hindered settling factor, $R(\phi)$, to quantify the strength of a particle network in compression and the inter-phase drag respectively, and linking it to other theories and related de-watering parameters available in the literature. The links between behaviour of a concentrated particle system in shear and compression are then discussed and a review of the various experimental methods available for determination of the de-watering parameters is presented. The final section overviews the practical application, benefits and limitations of models for real de-watering processes.

KEYWORDS: Filtration; Sedimentation; Thickening; Consolidation; Permeability; Compressibility; Centrifugation; Yield stress.

1. INTRODUCTION

The term "Compressive Rheology" is a relatively recent term used to describe the behaviour of twin-phase systems of, generally, particles of solids in liquid under the influence of compressive rather than shear forces. Compressive rheology formally emerged from the work of Buscall and White [1] based on their fluid mechanical approach to the uniaxial yielding and subsequent consolidation of networked particles under a compressive force. This area of study is critical for applications as diverse as filtration and centrifugation of suspensions in the mineral and water treatment industries to disposal of tailings in an impoundment or the characterisation of clay sediments for civil engineering applications. As a result of this, numerous approaches to the same problem domain have emerged independently or in parallel in various disparate scientific disciplines over the past 50 years, albeit based on the same fundamentals.

The main criteria that must be satisfied for measurement of compressive rheology is that a sufficient particle concentration must exist in the system such that inter-particle interactions within the system cause a continuous network to form and this network is subject to uniaxial compression. The particle network has an integral strength which, as is the case in the shear of concentrated suspensions, must yield for deformation to occur. However, contrary to yielding in shear, the field of compressive rheology is concerned with the subsequent expulsion of fluid from the network after yielding, leading to an increase in the concentration of the particle network via consolidation and de-watering. To describe the kinetics of the consolidation process requires, in addition to the strength of the network, a measure of the rate of escape of liquid during consolidation, which is in turn controlled by some measure of the permeability of the network to fluid flow. In the Buscall-White [1] theory the strength of a network is characterised by a compressive yield stress, $Py(\phi)$ and the permeability by an interphase drag parameter called the hindered settling factor, $r(\phi)$.

Due to the practical inter-dependence of behaviour of un-networked and networked systems, generally the study of the compressive rheology also requires investigation of the de-watering / sedimentation behaviour of the dilute, un-networked system. Hence compressive rheology broadly refers to the study and measurement of the de-watering / consolidation behaviour of solid-liquid systems ranging from dilute up to fully networked solids concentrations.

The purpose of this article is to review the subject area including a reconciliation of the different approaches and the characteristic parameters utilised in each and a coverage of experimental methods available for their determination. Fundamental aspects of the effect of network structure and inter-particle forces and the link between behaviour in shear and compression will also be discussed. Finally, practical aspects of the application of compressive de-watering theory to filtration and sedimentation under gravity or a centrifugal field will be covered.

2. THEORY

Initially only the theoretical framework for the Buscall-White [1] formulation of the problem will be discussed along with its related parameters. Later, parallel theories and parameters will be discussed in terms of how they inter-relate with the Buscall-White approach.

As mentioned previously, there are two key properties, the compressibility and the permeability, used to describe the behaviour of sediments under compressive forces. These arise from the consideration of the fluid mechanics and force balances relevant in a solid-liquid system undergoing concentration via an applied force which may be either through gravitational, osmotic or positive / negative (vacuum) pressure means. Whilst the engineering unit operations designed to exploit these de-watering forces are varied in design, the fundamental concepts, and hence the governing mechanics are the same in each case involving the concentration of solids from an initial (assumed homogenous) concentration which may or may not be initially networked, via relative movement of the solid and liquid phases past one another. The consideration of an initially un-networked system requires concurrent treatment of the behaviour of suspensions undergoing de-watering in the dilute solids concentration
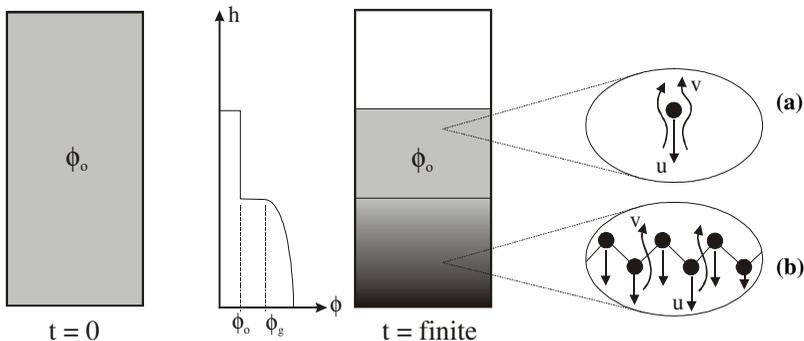
Figure 1: Schematic of a sedimentation process showing basic consolidation mechanisms and relative solid and liquid velocities (u and v respectively) for: (a) a dilute region and (b) a volume element of a networked sediment.

regime (where compressive effects are negligible) and presents a logical starting point for the development of theory.

Figure 1 simplistically illustrates the sedimentation of a system in a vessel from an initially homogenous, low initial solids concentration, ϕ_o, which can be considered as dilute and un-networked. At some finite time the particles will have settled under gravity forming a bed which has a concentration gradient from a maximum at the base up to a characteristic volume fraction, the gel point, ϕ_g at the top of the sediment. Above the top of the sediment, the volume fraction will be unchanged from ϕ_o and further upwards lies a clear liquid region. In order to discuss the theory it is useful to consider the conceptual transitions in the behaviour of the solid-liquid system as the frame of reference is moved from the suspension at the initial state downwards into the bed.

Figure 1(a) illustrates the situation for an isolated particle where the particle has a settling velocity **u** and displacement of fluid causes fluid motion in the opposite direction, **v**. The major forces acting on this particle (ignoring diffusional motion) will be the hydrodynamic / inter-phase drag force, **F_d**, and the gravitational or buoyancy force, **F_g**, which can be together balanced giving:

$$(u-v) = \frac{\Delta\rho \, g V_p}{\lambda \eta a_p}.$$ ....(1)

where $\Delta\rho$ is the density difference between the solid and liquid, g is the gravitational field, V_p is the volume of the particle, λ, is the Stokes settling coefficient, η, is the liquid viscosity and a_p is the particle diameter.

If the particle concentration is increased in this free settling region, hydrodynamic interactions between particles also increase, leading to a deviation from

Stokes settling behaviour. These interactions can be accounted for by a volume fraction dependent hindered settling factor, $r(\phi)$. Landman and White [2] define $r(\phi)$ through the following equation for the settling velocity, $u(\phi)$:

$$u(\phi) = \frac{u_0(1-\phi)^2}{r(\phi)} \qquad \ldots\ldots\ldots(2)$$

where u_0 is the settling velocity of a single particle in an infinite media (Stokes law for spherical particles).[1] At the infinite dilution limit, $\phi \rightarrow 0$, particles are unaffected by neighbouring particles, thus $r(\phi) \rightarrow 1$. As the concentration increases, hydrodynamic interactions between particles hinder the settling velocity and $r(\phi)$ increases exponentially. The upper limit is $r(\phi) \rightarrow \infty$ as $\phi \rightarrow 1$. This limit is never reached in practice due to the existence of a maximum close packed concentration ($\phi_{cp} \approx 0.64$ for random monodisperse hard spheres). The hindered settling function is thus always finite and characterises the consolidation rate of the suspension at all concentrations.

The name of this function is thus somewhat misleading since it is effectively a drag factor which not only characterises hydrodynamic drag in hindered settling, but also in the consolidation or flow through a particle network. Hence $r(\phi)$ may be used to quantify hydrodynamic drag associated with flow through filter cake compacts. In this high solids region, the hindered settling function may be thought of as an inverse function of the permeability with, rather than solids moving through a continuum of liquid, the liquid permeating through a bed of solids.

As the frame of reference is moved further downwards the particle concentration jumps to the gel point, ϕ_g at the top of the sediment. This corresponds to the point where interparticle forces or direct particle contact result in a spanning particle network filling the containing vessel. This is sometimes termed the percolation threshold or critical concentration, ϕ_c. At this point the interactions between the particles resist gravity and compression. The existence of a network results in the requirement of a network stress term in the force balance, F_c, in addition to the gravity / buoyancy and hydrodynamic drag forces, F_g and F_d respectively. The network stress term is related to a particle pressure, P_s, which equates to the elastic stress in the particle network for flocculated or coagulated systems or to the osmotic pressure of the particles, $P_{os}(\phi)$, for stable particle systems or systems below ϕ_g.

Due to the particle pressure it is necessary to determine a force balance on a volume element of suspension rather than an individual particle (figure 1b). A one-dimensional force balance in the vertical downward (z) direction (i.e., in the direction of g) on a volume element of suspension, at concentration ϕ, is derived for the solid phase assuming inertial, bulk and wall shear forces are negligible [3, 4].

$$-\frac{\lambda}{V_p}\frac{\phi r(\phi)}{(1-\phi)}(u-v) - \frac{\partial P_s}{\partial z} - \Delta\rho\phi g = 0 \cdot \qquad \ldots\ldots\ldots(3)$$

---

[1] Note that Buscall and White [1] describe u(ϕ) without the square on the (1 - ϕ) due to a slightly different form of the original force balance.

The combination of the above force balance and continuity equations for the solid and liquid allow modelling of the consolidation process however full solution of the problem requires a constitutive equation relating the particle pressure, P_s, to ϕ and u.

For a stable suspension, the particle pressure equates simply to the osmotic pressure of the suspension, $P_{os}(\phi)$, as mentioned previously, which can be measured directly [5]. Stable suspensions will consolidate to form dense beds with concentrations approaching the close packing limit, ϕ_{cp}.

However, for a suspension of particles interacting with an attractive net energy (eg. through electrostatics or bridging flocculation) the particle pressure must be characterised by a physically measurable network strength which depends on the local volume fraction of solids, ϕ. This strength is defined as the compressive yield stress, $P_y(\phi)$ [1]. An element of the network at a given volume fraction, ϕ, will remain in its original form until an applied stress, ΔP, on the network exceeds the compressive yield stress at that solids concentration. At this stage, the structure of the network will collapse, particle consolidation will occur and the local volume fraction will increase [1].

The $P_y(\phi)$ function depends implicitly on the properties of the suspension network structure, that is, the number, strength and arrangement of inter-particle bonds. The structure is determined by the flocculation or coagulation state, any surface active additives, and any previous shear or compression history of the suspension. Clearly, $P_y(\phi)$ will increase with ϕ as the number of inter-particle linkages increases, so de-watering occurs until ϕ is such that $P_y(\phi) = \Delta P$. $P_y(\phi)$ can only be traced in a regime where ϕ is greater than ϕ_g and approaches infinity for $\phi \to \phi_{cp}$. For $\phi < \phi_g$, the particle concentration is too small to allow a particle network to develop and thus the compressive yield stress is zero (neglecting the suspension osmotic pressure).

The assumption of equivalence of the compressive yield stress to P_s in the sediment force balance requires that the dynamics of the yielding process are considered. Buscall and White [1] proposed the following constitutive equation for interacting particle systems to describe the dynamics of consolidation:

$$\frac{D\phi}{Dt} = \begin{cases} 0 & , \quad P_s < P_y(\phi) \\ \kappa(\phi)\left[P_s - P_y(\phi)\right] & , \quad P_s > P_y(\phi) \end{cases} \qquad \text{.........(4)}$$

where $D\phi/Dt$ is the material derivative of the local concentration, and $\kappa(\phi)$ is a rate constant called the dynamic compressibility. Equation (4) formally states that the network resists compression if $P_s < P_y(\phi)$, but collapses if $P_s > P_y(\phi)$.

Buscall and White [1] argue that if the drainage of the fluid is the rate determining step in the dynamics of collapse, then $\kappa(\phi)$ is of order $O(\phi/\eta)$, where η is the fluid viscosity [6, 1]. For this case, estimating the order of the terms in equation (4) gives

$$P_s = P_y(\phi)\left[1 - O(a_p^2 / h_0^2)\right] \qquad \text{.........(5)}$$

where a_p is the particle size and h_0 is the container size.

Typically, $O(a_p^2 / h_0^2) \sim (10^{-12} - 10^{-8})$, and therefore equation (4) can be replaced by:

$$P_s(z,t) = P_y[\phi(z,t)] \qquad \text{.........(6)}$$

in the networked region. The compressive yield stress can thus be treated as a direct measure of the particle pressure or the strength of bonds between particles in an attractively interacting particle suspension under compression.

An important consideration for the use of equation (6) is the assumption that compression is irreversible (since the pressure completely characterises the local concentration), which will not be applicable for investigation of viscoelastic systems. This equation is only strictly valid for strongly flocculated systems possessing a contiguous space-filling network structure but this has proven to be a reasonable assumption for many systems.

Thus, the force balance and the solid and liquid phase continuity equations combined with the compressive yield stress function, $P_y(\phi)$, and the hindered settling factor, $r(\phi)$ a complete description of a consolidation process is possible.

Note that, as it appears in the force balance, $r(\phi)$, is invariably linked to the quantity λ/V_p and in terms of measuring $r(\phi)$ experimentally (see later), unless the exact dimensions of the particles in the system are known, it is impossible to explicitly determine $r(\phi)$ itself. Given that most real (industrial) systems encountered are poly-disperse, the fact that the actual characteristic size of an aggregate or floc in an interacting particle system is seldom known and that these aggregates or flocs are of unknown shape it is more convenient to simply measure the entire quantity $\dfrac{\lambda}{V_p} r(\phi)$

experimentally. This is denoted $R(\phi)$ and referred to as the hindered settling function, particularly in recent literature on the subject [7, 8].

The basic consolidation equations described by Buscall and White have been adapted to describe a variety of de-watering situations including thickening and sedimentation processes [4, 9], centrifugation [10, 1, 11, 12] and filtration [13, 14,15, 16, 7]. Details and application of these theoretical frameworks to both laboratory and practical studies will be discussed later.

At this point a further de-waterability parameter should be introduced which comes from the treatment of the filtration problem and the development of a diffusion equation for the local volume fraction [17, 15, 16] namely:

$$\frac{\partial \phi}{\partial t} = \frac{\partial}{\partial z}\left(D(\phi)\frac{\partial \phi}{\partial z} - \phi\frac{dh}{dt}\right) \qquad \text{.........(7)}$$

where dh/dt is the rate of movement of either the piston or surface of pooled feed suspension above a filter membrane and $D(\phi)$ is the filtration solids diffusivity defined as:

$$D(\phi) = \left[\frac{\delta P_y(\phi)/\delta(\phi)}{R(\phi)} \right](1-\phi_\infty)^2 \qquad \ldots\ldots\ldots(8)$$

This parameter can be thought of as an effective diffusion coefficient for the solid phase and can be seen to encompass both the compressibility of the network and the hindered settling function, quantifying the permeability. As a comparative tool for investigating the dewaterability of different materials, comparison of the functionality of $D(\phi)$ over the range of volume fractions of interest in a de-watering operation reveals the material that will de-water faster. Methods for the determination of $D(\phi)$ have been detailed in the literature [18, 19].

Parallel Theories and Related Parameters

The derivation of the force balances described in the previous section is not unique to the work of Buscall and White. Similar theories have been developed in a number of other fields of research. The two main areas where equivalent theories of compressive rheology have emerged are in solid-liquid separation modelling, specifically the areas of filtration and thickening and in the fields of civil and geotechnical engineering. Given the same fundamental basis, the modelling equations, the parameters used and the techniques utilised to measure them can be shown to be related, in many cases by very simple relations. The purpose of this section of the review is to describe the main approaches and to reconcile similarities and differences between them.

Due to the importance of the need to model and quantify the behaviour of compacted clay beds in geotechnical engineering, the first detailed treatment of consolidation came from Terzaghi and Peck [20] who used a hydraulic conductivity, k, and a coefficient of volume compressibility, m_v, to characterise the permeability and compressibility behaviour of a sediment. The hydraulic conductivity is equivalent to a Darcian permeability and m_v is related to the effective solids stress, σ', via:

$$m_v = -\frac{1}{1+e_0}\frac{de}{d\sigma'} \qquad \ldots\ldots\ldots(9)$$

where e_0 is the initial void ratio of the sediment prior to compression. The Terzaghi theory utilises these measures of permeability and compressibility combined in a coefficient of consolidation, c_v, defined as:

$$c_v = \frac{k}{m_v \rho_l g} \qquad \ldots\ldots\ldots(10)$$

The original theory of Terzaghi assumes that k and m_v, and hence c_v are constant throughout consolidation which can lead to errors, especially for large strain deformations and as a result extensions to the model have been made by various authors [eg. 21]. Despite this, c_v is still often measured and used as a quantification of compressional kinetics.

It has been shown that the refined geotechnical approach proposed by Gibson et al. [21] which uses a Lagrangian, material coordinate formulation, can be directly transformed to give equivalent governing equations to those of the Buscall White approach [12] by substituting $R(\phi)$ for k and $P_y(\phi)$ for σ. It has also recently been demonstrated that c_v and the filtration diffusivity, $D(\phi)$ are simply related via [22]:

$$c_v = \left(\frac{\phi}{\phi_0} \right) D(\phi) \qquad \text{..........(11)}$$

where ϕ is the volume fraction at the end of consolidation. The advantages from this work are the ability to interchangeably utilise data and the possibly more theoretically rigorous test methods developed in filtration for geotechnical use and vice versa.

Another area that has made key contributions to development of consolidation theory has been in filtration research. The classic work of Tiller and co-workers over the past 50 years has used two key parameters to model the cake formation and compression stages of filtration from suspension [23, 24, 25, 26], the specific cake resistance, α, and the solids pressure, p_s. The origins of the specific cake resistance come from the original treatment of filtration mechanics by Ruth [27] based on a Darcian approach.

A key conceptual difference exists between the traditional filtration approach and that of Buscall and White in that the two quantities, specific cake resistance and solids pressure, have been defined from within the modelling domain of filtration processes rather than as general "material properties" defined independently of their application. As a result, rather than focussing on the concept that a material has a characteristic $P_y(\phi)$ property, p_s, is not generally talked of as a material property and is more often referred to as the void fraction versus solids pressure (p_s vs. ε) relationship. Similarly the concept of permeability as a material characteristic is not strong in this approach as is indicated by the convention of reporting specific cake resistance data as a function of applied pressure, of which it is only an implicit function defined by the mechanical conditions in question, rather than solids concentration, of which it is an explicit function under all conditions. Furthermore, this approach precludes the definition of specific cake resistance in a non-networked environment, further reducing its generality. In spite of the obvious links in fundamental quantities between sedimentation, filtration and centrifugation, only a few papers exist explicitly focussing on linking the solids pressure and the specific cake resistance parameters from filtration to all modes of compressive de-watering [28, 29].

Despite of these conceptual differences, the underlying fundamental quantities modelled by each of the p_s vs. ε relationship and the specific cake resistance can be directly related to the Buscall-White parameters. The p_s vs. ε relationship is identical to $P_y(\phi)$ in the Buscall-White approach. Additionally, the specific cake resistance can be related to the hindered settling function via the Darcian permeability, k, by equating the liquid phase force balances using k and $R(\phi)$ for the condition of flow through an incompressible packed bed, ignoring gravitational forces:

$$\frac{\phi}{(1-\phi)} R(\phi) v = \frac{dP_l}{dz} \qquad \text{..........(13)}$$

$$v = \frac{k}{\eta} \frac{dP_l}{dz} \qquad \ldots\ldots\ldots(14)$$

where v is the flow velocity of liquid through the bed, which leads to:

$$k = \frac{\eta(1 - \phi)}{\phi R(\phi)} \qquad \ldots\ldots\ldots(15)$$

Equation (13) is the Hindered Settling Force Balance and equation 14 is the Darcian Force Balance.

Based on the definitions of the specific cake resistance [30] this then leads to:

$$\alpha_m = \frac{R(\phi)}{(1 - \phi)\rho_s \eta} \qquad \ldots\ldots\ldots(16)$$

for a mass specific cake resistance or for a volume specific cake resistance this gives the following:

$$\alpha_v = \frac{R(\phi)}{(1 - \phi)\eta} \qquad \ldots\ldots\ldots(17)$$

Use of these relationships then allows conversion of the wealth of published data for specific cake resistance into hindered settling function data and vice versa.

Note that the analytical approach to the modelling of the cake compression phase of a filtration operation used in traditional filtration literature is based on the Terzaghi model of consolidation of a networked suspension [31]. This was refined for application to filtration by Shirato [32, 33]. As it is based on the geotechnical approach and characterises the consolidation process using a consolidation coefficient, C_e, the same inter- relationships between the Buscall-White parameters and the consolidation coefficient apply, as discussed earlier.

There are other approaches to modelling of compressive de-watering operations which differ slightly in nomenclature to the Buscall-White approach but have a similar, rheological basis. An example of this is from the work of Bürger, Concha and co-workers who have utilised a similar framework to Buscall and White for the modelling of sedimentation processes [34, 35], continuous thickeners [36] and centrifuges [37]. In their work they utilise the effective solids stress, $\sigma_e(\phi)$, as the numerical equivalent to $P_y(\phi)$ and the Kynch batch flux density function, f_{bk}, as an equivalent to $R(\phi)$ which is defined as follows [35]:

$$f_{bk} = \frac{\Delta\rho g \phi^2 (1 - \phi)^2}{\alpha(\phi)} \qquad \ldots\ldots\ldots(18)$$

where $\alpha(\phi)$ is the resistance coefficient (different to the specific resistance in filtration literature) giving:

$$f_{bk} = \frac{\Delta\rho g \phi (1 - \phi)^2}{R(\phi)} \qquad \ldots\ldots\ldots(19)$$

Shear versus Compression

The yielding behaviour of a networked particulate structure under compression is expected to be related to that in shear given that the fundamental basis of both is the ability of the network to accommodate elastic strain. Consequently, exploring the links between shear and compressive yielding has been the subject of a number of studies [38, 39, 40, 41, 42, 43].

It should be pointed out that the existence of a shear yield stress, τ_y, has been much debated by various authors. At times it has been referred to as a "myth" [44], "an engineering reality" [45], "empirical" [46] or "apparent" [47]. The prime reasoning for the non-existence of the shear yield stress is based on comparison of the time-scale of observation relative to the time scale of relaxation of the network and the observation that flow will be observed on much longer time scales for stresses below a yield stress determined in a short time scale measurement. Chang et al. [48], as has been the case in other work, noted that the magnitude of the yield stress determined was dependent on the rate of application of the stress. It is this reasoning that results in labelling the yield stress "an engineering reality" as, on the time scale of typical engineering processes, materials behave as if they have a true yield stress [45].

Whilst such a debate has not surrounded the existence of a compressive yield stress, there is limited evidence suggesting that its existence also may not be so clear cut. Wakeman and Tarleton [31] express some concerns over the concept of ϕ_g acting as a sharp de-lineation point between a fluid-like system and a load-bearing network. Additionally, a number of workers have observed sedimentation behaviour of systems where consolidation of the network has been observed at solids stress conditions *below* the compressive yield stress of the material at the local volume fraction [49, 12] for coagulated octadecyl-coated silica spheres in hexadecane and fine clay tailings. The current authors note also that unpublished sedimentation results on strongly coagulated zirconia suspensions, conducted on an optical table to minimise vibrations, yielded similar observations. Shen et al. [49] propose that a stress-induced creep mechanism may be operative over long timescales which may result in apparent yielding of a network at stresses below the local $P_y(\phi)$. The authors are unsure if any detailed studies confirming or discounting the existence of this creep phenomenon have been conducted.

Whether or not a true yield stress exists in shear or in compression the importance of both quantities and their inter-relationship, for both research and application, has lead to a number of studies being conducted in the area. A very good recent overview of these studies was provided by Zhou [50] and this will be summarised here.

It has been well documented that the shear yield stress is a macroscopic manifestation of the strength of interparticle forces in a particulate network and its microstructure [eg. 51, 52]. Previous work on metal oxide systems has demonstrated that the yield stress is a strong function of the electrostatic repulsion between particles and is a maximum at the Isoelectric point (IEP) or point of zero charge, where attractive van der Waals forces dominate and the system is strongly flocculated [eg. 53, 54, 52]. At pH's on either side of the IEP the degree of electrostatic repulsion

increases and the shear yield stress is observed to gradually decrease towards zero for the case of completely dispersed systems.

Based on a model by Kapur et al. [55], Scales et al. [56] proposed a general interactive model for the shear yield stress of a flocculated suspension of mono-disperse particles based on a summation of pairwise interactions calculated from DLVO theory:

$$\tau_y = \frac{0.022}{\pi d} \phi K(\phi) \left[\frac{A}{H^2} - \frac{24\pi D \varepsilon_o \kappa \zeta^2}{(1 + e^{\kappa h_o})} \right] \qquad \ldots\ldots\ldots(20)$$

where $K(\phi)$ is the mean coordination number, d is the diameter of the particles and the terms inside the brackets account for the van de Waals and electrical double layer interaction forces. The model was shown to accurately describe the yield stress behaviour of flocculated alumina suspensions, assuming that the coordination number and mean interparticle separation, H were adjusted to allow the model to fit the data. The model is not truly predictive in this respect but does allow significant observations of the scaling behaviour of the yield stress with particle size, volume fraction and interparticle forces.

Scales et al. [56] removed the effect of particle size and volume fraction from the model equation by scaling data with the maximum yield stress which occurs at a zeta potential, ζ, of zero such that:

$$\frac{\tau_y}{\tau_{y\,max}} = 1 - \frac{24\pi\varepsilon\kappa\zeta^2 H^2}{A(1 + e^{\kappa H})} \qquad \ldots\ldots\ldots(21)$$

Equation (21) predicts a single linear relation between the normalised yield stress and the square of the zeta potential irrespective of particle size and this has been observed for mono-disperse alumina particles of varied particle sizes [43]. The slope of this plot can yield the mean inter-particle separation and the validity of this relation experimentally implies that DLVO theory, through the strength of individual inter-particle interactions, can accurately characterise the impact of changing surface chemical conditions on suspension rheology. Zhou [43] also extended this approach to scale normalised viscosity data.

Based on the consideration that yielding in compression is dependent on the same fundamental network properties as yielding in shear, a number of workers have applied similar scaling to compressive yield stress data [57, 50]. Data presented in figure 2, taken from Green [57], for a zirconia suspension demonstrate that the same scaling of the normalised shear yield stress can be applied to the compressive yield stress.

The effect of particle size on the shear yield stress predicted by equation (21) is an inverse dependency, however numerous workers have demonstrated that in practice an inverse–square dependency exists [39, 51, 58, 43]. The origins of the extra inverse dependence of the shear yield stress on particle size is unknown but it is unlikely to come from the DLVO terms which have been shown to adequately model the force dependencies. It is more likely to arise from coordination and structural variations.
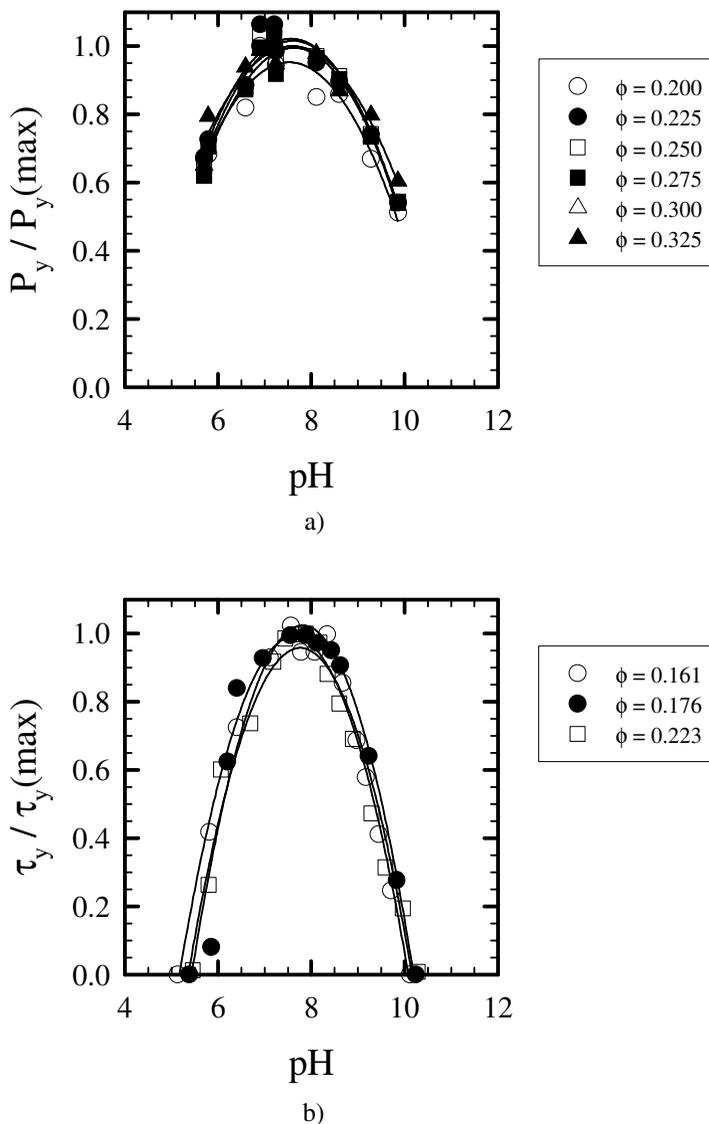
Figure 2: Normalised shear and compressive behaviour of zirconia suspensions as a function of pH and solids concentration. (zirconia, 0.01M KNO$_3$) (adapted from Green, [57]). **a)** Plot of normalised P$_y$. **b)** Plot of normalised τ_y.
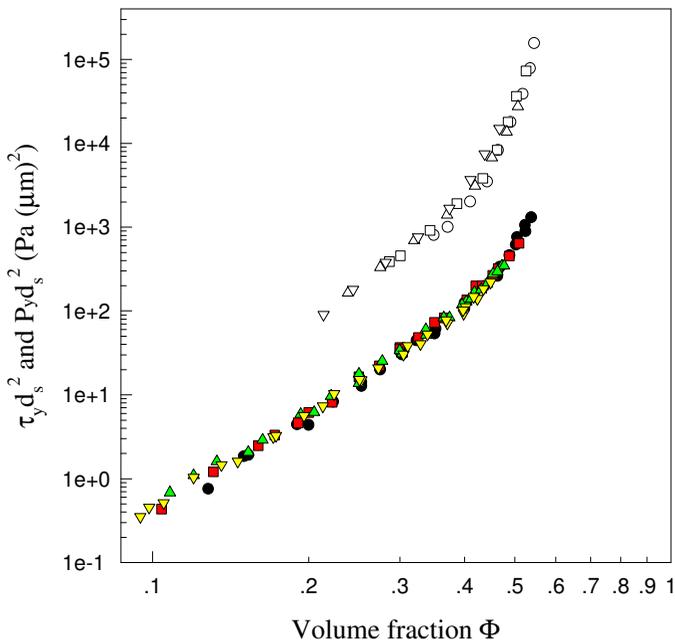
Figure 3: The comparison of compressive and shear yield stresses in terms of $\tau_y(\phi)d_s^2$ and $P_y(\phi)d_s^2$ as a function of volume fraction for four alumina particles at pH 9.0 ± 0.2, AKP-15 ▼▽ ; AKP-20 ○● ; AKP-30 □■ ; AKP-50 △▲ ; solid symbols shear yield stress, empty symbols compressive yield stress (adapted from Zhou et al. [43])

Data taken from Zhou et al. [43] presented in figure 2 clearly indicates that the application of this inverse-square scaling to compressive yield stress data for alumina suspensions of varying particle size also holds true, again indicating the link between behaviour in compression and shear.

Both figures 2 and 3 indicate that the magnitude of the compressive yield stress exceeds that of the shear yield stress. This has been the case in all studies comparing the two properties, however the observed relationship between them varies significantly across these studies. Shin and Dick [59] compared $P_y(\phi)$ and $\tau_y(\phi)$ for water treatment sludges and observed a linear relationship between the two. In contrast, Buscall et al [38] compared $P_y(\phi)$ and $\tau_y(\phi)$ for flocculated latex and observed and approximately constant ratio for $P_y(\phi)/\tau_y(\phi)$ of 55 and later observed a ratio of 100 for silica particles. Meeten [40] obtained a constant ratio of 11 for a bentonite

suspension and Green [57] obtained a constant ratio of 15 for zirconia but did not detect a constant ratio for titania, possibly due to limited overlap between the solids concentrations at which $P_y(\phi)$ and $\tau_y(\phi)$ data were available.

Zhou [50] also investigated the ratio $P_y(\phi)/\tau_y(\phi)$ for titania and different particle sized alumina and obtained a constant ratio of 29 and 14 respectively at low volume fractions but observed that the ratio then increased linearly with volume fraction above a critical volume fraction of around 0.4 for both materials (indicated in figure 3 for the alumina system). These results suggest that at some critical packing density $P_y(\phi)$ becomes a stronger function of ϕ.

The studies of Channell and Zukoski [42] and also Zhou [50] both investigated $P_y(\phi)$ and $\tau_y(\phi)$ for flocculated alumina suspensions from the same supplier and of the same particle size. Channell and Zukoski obtained a constant ratio for $P_y(\phi)/\tau_y(\phi)$ of 55 for their AKP-15 alumina in comparison to the figure of 14 obtained by Zhou [50]. The potential origins of this difference between the ratios was investigated by Zhou [50] who noted that, whilst the $P_y(\phi)$ data for both studies was similar, the $\tau_y(\phi)$ data obtained by Channell and Zukoski [42] were approximately 20% of the values he obtained. He concluded that this lower shear yield stress was most likely due to the different measurement techniques employed for $\tau_y(\phi)$ in the two studies – Zhou [50] used the vane technique [60] whereas Channell and Zukoski [42] used extrapolation of low shear rate data which can be influenced by slip phenomena at low shear rates. In addition, the effect of the slightly different preparation methods utilised in the two studies has also been documented to produce differences in shear yield stress [51]. All or any of these effects may be the cause of the difference between the data of Zhou [50] and Channell and Zukoski [42].

Explanations and models to account for the correlation between shear and compression have been proposed by various authors. Buscall et al. [38, 39] argue that if linear elastic models hold true, then the ratio $P_y(\phi)/\tau_y(\phi)$ will be constant. This is clearly the case for most materials investigated but appears to break down at higher volume fractions. Meeten [40] proposed a link between $P_y(\phi)$ and $\tau_y(\phi)$ via Poisson's Ratio, v, assuming linear elastic behaviour up to yielding (a condition known to be false for yielding in shear [eg. 61, 48]):

$$\frac{P_y(\phi)}{\tau_y(\phi)} = \frac{1-v}{1-2v} \qquad \ldots\ldots\ldots(22)$$

For the range of materials described in the literature, studies of compression and shear a value for Poisson's Ratio of between 0.474 and 0.497 is observed [50]. The value of equation (22) is limited due to the need to know the value of Poisson's ratio prior to any prediction of either $P_y(\phi)$ or $\tau_y(\phi)$ from each other and the high sensitivity of the relationship to small changes or errors in v.

A relationship between $P_y(\phi)$ and $\tau_y(\phi)$ can be derived from the work of Uriev and Ladyzhinsky [62] based on fractal structural considerations which yields the following relationship between $P_y(\phi)$ and $\tau_y(\phi)$:

$$\frac{P_y(\phi)}{\tau_y(\phi)} \approx \frac{a}{K_y H} \qquad\qquad\qquad \text{……….(23)}$$

where the coefficient, K_y, is expected to have a value of order 1 and H is the interparticle separation and a the particle size. This relationship exhibits the correct functionality in terms of the size of the ratio, which predicts $P_y(\phi)$ to be larger than $\tau_y(\phi)$ on the basis that the particle size is generally larger than the interparticle separation. However, the predicted dependence of the ratio on the particle size is contrary to the results of Zhou et al [43].

Kapur [63], using the shear yield stress model developed in Kapur et al [55] and Scales et al. [56], suggested that the failure of a network in compression occurs due initially to compression of particles closer to one another. Then, due to local heterogeneities and the directions of forces acting on the particles, the network becomes unstable and particles slip past one another into adjacent interstices to reach a new equilibrium state. This results in the measured compressive yield stress being essentially the shear yield stress of the network at the closest distance of approach of the particles, as determined by equation (20). If the closest distance of approach, H_c, is related to the average particle separation as:

$$H_c = \alpha H \qquad\qquad\qquad \text{……….(24)}$$

then the shear and compressive yield stresses can be related via:

$$P_y(\phi) = \alpha^2 \tau_y(\phi) \qquad\qquad\qquad \text{……….(25)}$$

The constant, α, is less than one and characterises the degree of compression of a bond before it breaks. Zhou [50] determined values for α of between 0.32 and 0.1 for the ratios of $P_y(\phi)$ to $\tau_y(\phi)$ in all of the literature studies mentioned previously.

Clearly from the number of studies conducted in the area there is a strong link between behaviour in shear and compression with an apparently straightforward, albeit system dependent, proportionality. Despite this, there has been limited detailed treatment of the nature of the yielding processes in shear and compression. It is expected that compressive yielding will be more complex than yielding in shear due to the added phenomena associated with densification of the network. The divergence in the proportionality constant observed by Zhou [50] above a critical solids concentration may be evidence of this, which he attributed to the presence of an enhanced geometric resistance which is manifest at high solids volume fractions in the compressive yield stress but not in the shear yield stress.

Of note also is recent work performed by Bowen and Jenner [64] and Koenders and Wakeman [65] who have endeavoured to take a similar approach to that taken by Kapur [63] to predict the solids pressure ($P_y(\phi)$) in a filter cake based on consideration of the pairwise interactions between particles. Bowen and Jenner [64] developed a full "physics to filtration" model of cake filtration with no adjustable parameters which demonstrated excellent agreement with data for a mono-disperse silica system with high levels of interparticle repulsion. They related the solids pressure in the cake, p_s, to the disjoining pressure, p_d, which incorporated the combined effects of electrostatic double layer, van der Waals and hydration forces, similar to the approach in Kapur

[63]. Unfortunately, the theory is limited to mono-disperse systems and, more significantly, due to the assumption of close packing in the cake, the theory becomes inapplicable for attractively interacting particle suspensions. In this situation the interparticle separation cannot be determined with great confidence *a priori*. It should be noted that for flocculated systems, Kapur et al. [55] use a volume fraction dependent coordination number (see equation (20)) to quantify the structure of the cake and the interparticle spacing used acts as a fitting parameter.

Koenders and Wakeman [65] proposed an alternative approach whereby the solids pressure, p_s, is related solely to the double layer force only and attempt to model the intra-cake stresses based on pairwise summation of these interactions. The approach yielded some valuable information regarding the effect of zeta potential on filtration, albeit only for limiting situations. A significant limitation of this and the work of Bowen and Jenner [64] is that the modelling of the solids pressure, p_s, and its comparison with real data is conducted only within the framework of a filtration process. No independent validation of the ability of the models to predict p_s as a function of particle size, surface chemical conditions, structure or solids concentration is completed and ultimately this is the key to the ability to predict p_s or $P_y(\phi)$ from first principles.

2.   CHARACTERISATION   OF   COMPRESSIVE   RHEOLOGICAL PARAMETERS

Having established the formal links between the de-watering parameters utilised in the Buscall-White approach to de-watering and the other approaches detailed in literature, the number of documented characterisation techniques available for $P_y(\phi)$ and $R(\phi)$ then becomes massive. Listing of all of these approaches is not feasible, however the main types that have been established for measurement of the de-watering parameters will be examined.

In addition, given the changing dynamic of research worldwide in its more explicit corporate focus, development of practically applicable techniques suitable for industrial modelling and optimisation work is increasingly required. In spite of the wealth of detailed studies on model systems and application of modelling approaches in a laboratory environment, invariably, the compressive de-watering approaches applied in practical situations are non-rigorous and somewhat empirical. Examples of this are documented in the geotechnical field [22] and also in filtration design and optimisation [31].

One of the main barriers in the past to the widespread use of rigorous modelling approaches has been the difficulty in obtaining the de-watering parameters required as model inputs. An example of this is the formally documented techniques for the determination of $P_y(\phi)$, $R(\phi)$. Centrifuge techniques exist and were refined for the measurement of $P_y(\phi)$ [66,11] however they are relatively slow and were limited in their ability to provide a measure of $R(\phi)$. Later, Green et al. [67] developed a constant pressure filtration technique that measures both $P_y(\phi)$ and $R(\phi)$, although the full characterisation of a material was still slow. This was on par with most other filtration techniques developed in the filtration literature [eg. 68] but further refinement of the

testing approach has yielded improvements in the speed of characterisation through stepped pressure filtration testing [7, 8].

In conjunction with the need to develop faster characterisation techniques for practical application of compressive de-watering theory is the need to improve the range of solids concentrations over which data may be readily determined along with the accuracy of the data. Tien [69] notes, relevant to the filtration literature, that a significant amount of effort needs to be focussed on, rather than the models themselves, the determination of the constitutive equations of the material parameters from experimental data. Such a focus, whilst worthwhile, needs also to embrace the fact that utilisation of rigorous models for de-watering processes requires de-watering parameter data at all solids concentrations from the feed up to the outlet solids concentration. Due to the size of this solids concentration range for many typical industrial systems, invariably there is no single technique that will determine the necessary data over the required concentration range. Hence, a range of techniques needs to be available and integrated into a general de-watering characterisation protocol.

Recent work by de Kretser et al. [70] has focussed explicitly on this integration. The results shown in figures 4 and 5 demonstrate full characterisation of $P_y(\phi)$ and $R(\phi)$ for a flocculated zirconia suspension from low to high solids concentrations. The results were obtained using a variety of techniques (to be described in the next sections) and clearly the agreement between them is very good. These results also demonstrate a significant drawback in the approaches of most research papers in the field of compressive de-watering, namely the assumption of a simplistic power-law type constitutive equation for $P_y(\phi)$ and $R(\phi)$. This can be assumed for de-watering processes running over a small concentration range, but would not be suitable in the case of, for example, a deep cone thickener fed at a low solids concentration, producing an underflow well in excess of the gel point.

The purpose of the preceding discussion has been to provide some background information relating to characterisation techniques and general issues associated with them. The actual testing approaches employed for ϕ_g, $P_y(\phi)$ and $R(\phi)$ will now be discussed.

Gel Point / Null Stress Solids

The gel point, ϕ_g, of a suspension alone is a useful parameter for gaining information regarding the nature of the compressibility and structure of sediments as well as being important in mathematical models of de-watering processes.

Direct determination of the gel point is not often completed, due in part to the difficulty of the measurement [69, 71]. As mentioned previously, ϕ_g is defined as the lowest solids concentration at which particles or flocs are able to form a self supporting network. If a sediment at the gel point is considered, due to the network structure, the weight of each individual floc or particle is transmitted down through the network and as a result, particles or flocs within a sediment are subject to compressive forces due to the self-weight of the overlying material. Hence material at the top of a bed will experience no compressive forces but, on moving a frame of observation

down through the bed, the compressive force increases with depth. The compressive force at the base of any sediment will thus be a maximum.
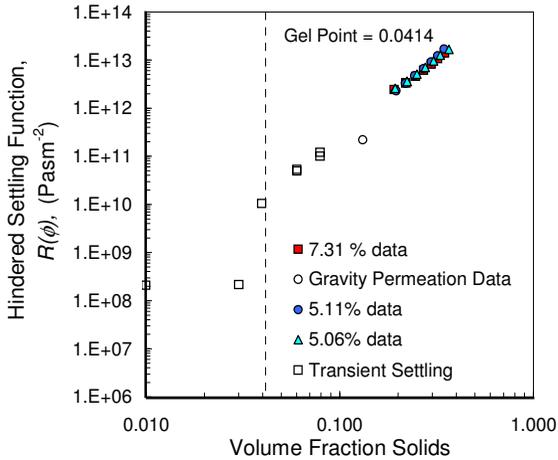

Figure 4: Example of results of full $R(\phi)$ characterisation of a coagulated zirconia suspension using filtration (different initial solids concentrations), permeation and transient batch sedimentation. (zirconia, pH 6.8, 0.01M KNO_3) (adapted from de Kretser et al.[70]).

The gel point can alternatively be thought of as the solids concentration of a networked suspension in the absence of any compressive force. As such, the solids concentration at the top of a sediment will be the gel point (provided the initial solids concentration, ϕ_o, was below ϕ_g). The difficulty in measuring this directly is that as soon as a bed network develops, the compressive forces present raise the average bed solids above ϕ_g, preventing its direct determination. Hence many researchers use alternate techniques.

Channell and Zukoski [42] used a simple technique where the data obtained for the compressive yield stress of alumina suspensions via filtration and centrifugation testing was fitted with a constitutive equation for $P_y(\phi)$ which effectively uses the gel point as a fitting parameter:

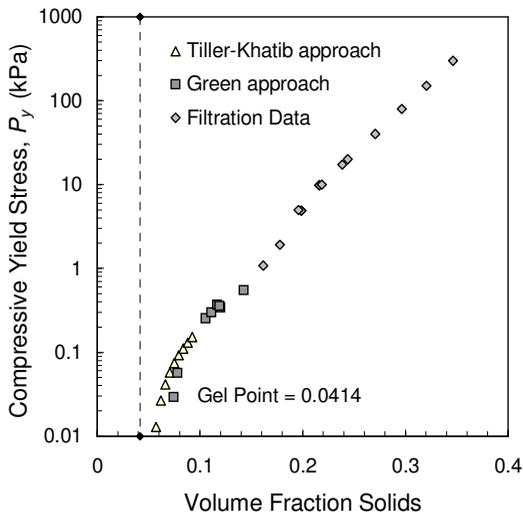$$P_y(\phi) = k\left(\left(\frac{\phi}{\phi_g}\right)^n - 1\right) \qquad \ldots\ldots\ldots(26)$$

Figure 5: Example of results of full $P_y(\phi)$ characterisation of a coagulated zirconia suspension using filtration and equilibrium batch sedimentation (zirconia, pH 6.8, 0.01M KNO$_3$) (adapted from de Kretser et al.[70])

The gel point determined via this technique was compared with average solids concentrations in sediments obtained from batch settling experiments with similar results. This fitting technique should be treated with caution, as the sensitivity of the fit to the value of ϕ_g is small. Obtaining a simple estimate of the gel point from a low initial height batch settling test at equilibrium is a far better initial estimate.

The observed and theoretical links between the behaviour of suspensions in compression and shear has lead a number of investigators to probe the behaviour of systems in shear to determine the gel transition point [eg. 72, 73]. Chen and Russel [72] probed the gel transition point of silica spheres grafted with octadecyl chains in an organic solvent at a range of temperatures through a combination of oscillatory rheological and light scattering techniques. The two approaches gave complimentary results. Unfortunately, there was no detailed study of the sedimentation behaviour of the system to correlate the shear and compressive properties.

Accurate measurement of the gel point via sedimentation requires compensation for the fact that as soon as particles or flocs form a network, the solids at the base of the network will experience a compressive force due to the weight of the overlying material. As a network is generally compressible, the compressive force acts to squeeze water out of the flocs, thereby concentrating the solids to a concentration higher than ϕ_g. Thus in settling experiments an element of suspension will *not*

necessarily stop falling and concentrating as soon as the gel point is reached. Settling will continue until some point and at which the compressive forces are balanced by the higher network strength of a more concentrated network and only then will settling stop. Under this condition, as the compressive force increases with depth in the bed, the strength of the network required to balance the compressive forces at each point also increases. Thus, the solids concentration in the settled bed will change with depth from ϕ_g at the top of the sediment to a higher, maximum value at the base of the sediment. Hence the average solids concentration in a sediment will always be higher than the gel point as some compression of the network will always occur due to the weight of solids present.

In order to properly measure the gel point, the solids concentration to which the flocs or particles settle in the absence of compression needs to be measured. The compressive pressure supplied at the base of a sediment, $P(0)$, due to the self weight can be calculated from:

$$P(0) = \Delta \rho g \phi_0 h_0 \qquad \qquad ....(27)$$

where ϕ_0 and h_0 are the initial solids concentration and height (m) of suspension at the commencement of the settling test. Equation (27) shows that as ϕ_0 and h_0 are changed, the maximum compressive force in the settled sediment also varies and thus so will the average sediment solids concentration, ϕ_{ave}. The key to calculating the gel point is determining the solids concentration of a sediment corresponding to $P(0)=0$. Thus equation (27) suggests that if settling tests are set up with a range of different $P(0)$, then a corresponding range of different ϕ_{ave} will result. By observing the relationship between $P(0)$ and ϕ_{ave}, extrapolation to the $P(0) = 0$ condition allows ϕ_{ave} in the absence of compression i.e. ϕ_g, to be determined. For measurement of the gel point, $P(0)$ can be varied by either holding ϕ_0 constant and changing h_0, h_0 constant and changing ϕ_0 or allowing both to vary. The condition of $P(0) = 0$ equates to extrapolation to either a zero value of ϕ_0, h_0 or the product $\phi_0 h_0$. This approach is detailed in de Kretser et al. (2002).

An alternative approach with a sound theoretical basis is presented both in Green [57] and Tiller and Khatib [71] based on the solution of the sediment force balance at equilibrium such that [74]:

$$\phi(h) = \frac{\partial w_c}{\partial h} \qquad \qquad ....(28)$$

which states that $\phi(h)$, the volume fraction of solids at any point h, below the top of a sediment is equal to the rate of change of w_c, the total volume of solids above point h, with depth below the top of the bed, h at equilibrium. This relationship allows the determination of the solids concentration at a given depth below the top of a sediment from a set of equilibrium batch settling tests, each starting with different total amounts of solids (as quantified by w_c which is equal to the product $\phi_0 h_0$). To use this relationship in determining the gel point equation (28) can be re-written as:

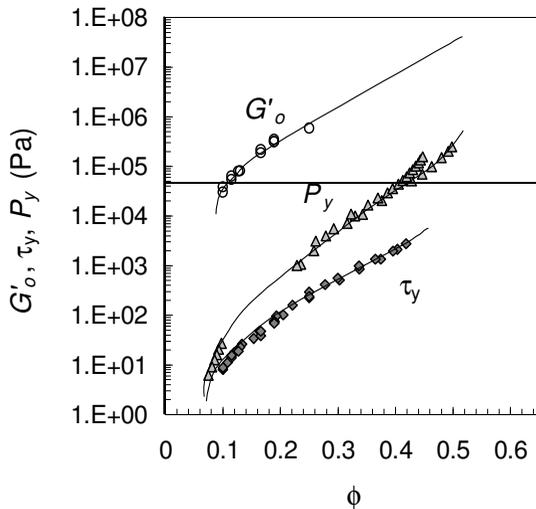$$\phi(0) = \frac{\partial (\phi_0 h_0)}{\partial h_\infty} \qquad \qquad ....(29)$$

Figure 6: Plot of G_o', τ_y and $P_y(\phi)$ versus ϕ for a coagulated alumina suspension (Sumitomo AKP30 alumina, pH 9, 0.01M KNO$_3$) (unpublished results from Aziz, A.A , University of Melbourne)

Thus the slope of a fit the $\phi_o h_o$ versus h_∞ data obtained from a sequence of settling tests will yield the solids concentration at a depth, h_∞ below the sediment surface. The gel point can thus be found from the slope of the fit at the point, $h_\infty = 0$, the solids concentration at the surface of the sediment.

Both of these approaches have been recently compared with favourable results [70] and they both suffer from the drawback that the extrapolation required from experimental data is a significant source of error. Whilst these approaches are probably the best available for determining the gel point, it is most likely that the true gel point will still be lower and a more detailed study on a model system utilising both shear and compressive techniques is required. Recent unpublished work by Aziz (2002 – unpublished data, University of Melbourne) for coagulated alumina suspensions is presented in figure 6 showing, on the one graph, the storage modulus, G_o', measured at a constant frequency and the shear and compressive yield stresses versus volume fraction solids.

Due to the logarithmic x-axis in this figure, the gel point will be expected to be an asymptote for $P_y(\phi)$ and τ_y and for G_o' a rapid drop off would also be expected as the gel point is approached. Clearly the results indicate remarkable correspondence between the gel point indicated by the different techniques, suggesting that the same value for ϕ_g can be predicted by quite independent approaches.

Characterisation of the Compressive Yield / Network Solids Stress

Techniques for the determination of $P_y(\phi)$ may be broadly distinguished into those using sedimentation and those using filtration. Centrifugal techniques are an extension of sedimentation methods. Each of these will be discussed in turn. The common theme of most of the approaches documented is that as $P_y(\phi)$ is an equilibrium quantity, they all involve compressing a sediment to an equilibrium state and either physically measuring or theoretically deriving the $P_y(\phi)$ data from the experimental results. It is also possible, utilising the existing theoretical models for transient behaviour of each of these test approaches, to extract $P_y(\phi)$ from non-equilibrium data, but this is generally not attempted.

The testing approaches listed here are the most common used for determination of the $P_y(\phi)$ or solids stress behaviour of a material. A number of other techniques have been proposed using the initial settling rate under a centrifugal field or the use of a pulse shearometer to measure the high frequency limit of the shear modulus, G_∞ [10, 75, 1], however they are as yet unverified in terms of their accuracy or suffer from severe limitations in terms of the practicality of application.

Compressive Yield / Network Solids Stress – Sedimentation and Centrifugation Techniques

$P_y(\phi)$ may simply be determined from equilibrium sedimentation tests using the same approach detailed for determination of the gel point i.e. equation (29). From the $\phi_o h_o$ versus h_∞ data obtained from a series of batch sedimentation tests, rather than determining the slope of the fit to the data at $h_\infty = 0$, the slope at any value of h_∞ will yield the volume fraction solids at that point. This can then be combined with the solids pressure at that point, determined by equation (27) to yield the $P_y(\phi)$ functionality at low solids concentrations. This approach is not often reported in the literature aside for the work in which it was developed [74, 71, 57]. As shown in figure 5, data obtained using this approach agrees well with that from filtration techniques.

A similar approach to the multiple equilibrium sedimentation tests described above is the multiple speed equilibrium sediment height technique proposed by Buscall and White [1]. This utilises a centrifuge to consolidate to equilibrium a sediment of material at each of a series of consecutively increasing gravitational fields. The initial experimental development of the technique was by de Guingand [76] and was refined further by Green et al. [66]. He evaluated the accuracy of the technique and proposed a new iterative mechanism for its application. It was concluded that for most practical applications the use of a mean value approximation for the determination of $P_y(\phi)$ from equilibrium sediment height data was sufficiently accurate. The mean value approximation allows determination of $P_y(\phi)$ via:

$$P(0) \approx \Delta\rho\phi_0 h_0 g\left(1 - \frac{h_\infty}{2R}\right) \qquad\qquad ……….(30)$$

$$\phi(0) \approx \frac{\phi_0 h_0 \left[1 - \frac{1}{2R} \left(h_\infty + g \frac{dh_\infty}{dg} \right) \right]}{\left[\left(h_\infty + g \frac{dh_\infty}{dg} \right) \left(1 - \frac{h_\infty}{R} \right) + \frac{h_\infty^2}{2R} \right]} \qquad \ldots\ldots\ldots(31)$$

$P(0)$ and $\phi(0)$ may thus be directly calculated for each (g, h_∞) raw data point using the above two equations for data determined in a centrifuge of radius, R. Determination of the derivative, $d\,h_\infty/dg$, at each point is all that is required.

This approach has been utilised in many published studies in the literature for various materials such as latex [39], cement paste [77], alumina [58, 42, 43], clay based-coal tailings [78], tar sands tailings [12] and zirconia [41]. In many of these studies the data obtained from the equilibrium sediment technique has been shown to agree with data obtained from other compressive yield stress determination techniques listed here. It should be noted that the use of a centrifugal field produces $P_y(\phi)$ data for solids concentrations well in excess of the gel point and potentially up to very high solids concentrations, depending on the centrifugal fields employed.

An alternative approach to the determination of $P_y(\phi)$ involves direct measurement of the solids concentration profile within a single compressed sediment at equilibrium rather than through evaluation of the response of a sediment to multiple compressive stress environments. The application of the compressive stress can either

be via gravity and the self-weight of the solids in the sediment or via application of an enhanced gravitational field in a centrifuge. Whilst a number of workers have measured concentration profiles in systems sedimenting under normal gravity [eg. 79, 80], this data is generally not used in the formal determination of $P_y(\phi)$ or any other measure of solids stress. The usual application of this approach is in sedimentation under centrifugal fields and further discussion will focus explicitly on this approach.

The theory for determination of $P_y(\phi)$ from an equilibrium concentration profile is defined by Buscall and McGowan [81], Auzerais, et al. [82], Bergström [83] and Bergström, et al. [11]. At equilibrium, integration of the force balance on a volume element of suspension in compressed sediment yields:

$$P_y(z) = \Delta\rho\omega^2 \int_0^z x\phi(x)dx \qquad \ldots\ldots\ldots(32)$$

where the origin of the x coordinate system is at the centre of the centrifuge. The compressive yield stress, $P_y(z)$, is equivalent to the cumulative weight of suspension above that point z. Thus to find the full compressive yield stress curve, the concentration profile must be progressively integrated from the top of the bed to the bottom for increasing values of z. This technique provides a more direct technique for the determination of $P_y(\phi)$ than the multiple speed equilibrium sediment height technique and is faster as it only requires centrifugation to equilibrium at one rotation speed. However, some method of measuring the concentration profile, $\phi(x)$, must be available for the centrifuged sample in order to calculate $P_y(\phi)$.

Non-invasive techniques for measurement of the concentration profile have been employed using γ-ray absorption measurements [83] and medical computer tomography (CT) scanning [82]. An alternative, somewhat laborious, but cheaper approach is the scraping of layers from the centrifuged sediment and measurement of the solids concentration of the scraped sediment. A similar technique has been used on filter cakes by Sherwood, et al. [84] and Meeten [85]. This approach was utilised by Green and Boger [41] and was shown to yield acceptable results within experimental error when compared to both the multiple speed equilibrium sediment height technique and a filtration technique (to be discussed in the next section). In each of these cases the integration of the concentration profile data is completed either graphically or through analytical or numerical integration of fitted curve to the experimental data. Green and Boger [41] observed that the quality of the calculated $P_y(\phi)$ data depended more on the quality of the raw data itself or the curve fit employed rather than the integration method used.

Compressive Yield / Network Solids Stress – Filtration Technique

Possibly the simplest measurement technique for $P_y(\phi)$ is utilising a standard constant pressure filtration, oedometer or compression-permeability (C-P) cell test. The principle of these measurements is that the sample to be tested is confined in a compression cell with a permeable membrane at one or both ends and is subjected to a uniaxial compressive force. On application of the pressure ΔP, the material filters and forms a cake which continues to de-water until a point at which it has a constant solids concentration, ϕ_∞ such that:

$$\Delta P = P_y(\phi_\infty)$$ ……….(33)

The final concentration is calculated either by:

$$\phi_\infty = \frac{\phi_0 h_0}{h_\infty}$$ ……….(34)

or by direct measurement on the cake produced in the test.

The pressure filtration technique has been used for some time in geomechanics to determine the solids stress of soils and has been a standard test in the filtration literature. Callaghan and Ottewill [86], Shirato, et al. [79], Meeten [40] and Sherwood and Meeten [87] have used a compression cell to examine the compressibility of clays. Grace [88] measured the solids pressure for a range of systems in a C-P cell. Recently, Miller, et al. [58] used pressure filtration to explicitly determine $P_y(\phi)$ for Al_2O_3 and ZrO_2 suspensions and Green and Boger [41] and Miller et al. [58] benchmarked the filtration techniques with centrifuge testing approaches. The beauty of the filtration approach is its simplicity and the absence of any numerical analysis. Its limitation is that each experiment only gives one $P_y(\phi)$ data point, requiring multiple tests to be performed in order to obtain the entire $P_y(\phi)$ curve.

Recently, a technique of applying consecutive pressure steps to the same sample has been developed and refined to the point where a single experiment allows determination of $P_y(\phi)$ in rapid time over a pressure range from 1 up to 400 kPa in an

automated filtration device [7]. This circumvents the problems with loading and testing multiple samples and significantly improves characterisation speeds. The high solids $P_y(\phi)$ data presented in figure 5 were determined using this technique. Clearly there is good agreement between the stepped pressure filtration data and the data from batch settling / ϕ_g analysis. The technique has been extensively used in recent industrial work on the thickening of Bayer process residues [89].

Characterisation of the Hindered Settling Function / Network Permeability

As with the measurement of $P_y(\phi)$, there are a number of broad categories of characterisation technique for $R(\phi)$. Significantly the existence of $R(\phi)$ as a finite quantity for un-networked systems means the characterisation techniques required must span the range of solids concentrations from effectively an isolated particle or aggregate up to a concentrated cake or compact. In the low to intermediate solids region the only testing methods available are sedimentation techniques. As the solids concentration increases through the gel point, centrifugal techniques are required. At high solids concentrations, permeation and filtration-based techniques have been developed to characterise $R(\phi)$. Each of these broad categories will be discussed in turn.

Hindered Settling Function / Network Permeability - Transient Sedimentation and Centrifugal Techniques

The very definition of the hindered settling function via equation (2) lends itself to a characterisation technique via measurement of the initial rate of fall of a suspension / supernatant interface for an un-networked system. However, it is possible to extend this approach to any system, networked or un-networked, settling under a normal gravitational field. Based on the original work of Buscall and White [1], Howells et al. [9] predict that for small times of sedimentation the following equation holds:

$$R(\phi_o) = \left(1 - \frac{P_y(\phi_o)}{\Delta\rho g \phi_o h_o}\right)\frac{\Delta\rho g (1-\phi_o)^2}{\hat{u}} \qquad\ldots\ldots\ldots(35)$$

Equation (35) suggests that, given a suspension's initial solids volume fraction, ϕ_o initial suspension height h_o, initial settling rate, $dh/dt = \hat{u}$ and solid-liquid density difference $\Delta\rho$, the hindered settling function, $R(\phi)$, can be determined, irrespective of whether the system starts sedimentation as a network or not. The term in the brackets associated with $P_y(\phi_o)$, the compressive yield stress of the starting material, accounts for the retarding effect of the existence of a network on the initial settling rate of the interface. In the event that ϕ_o is less than ϕ_g, then $P_y(\phi_o)$ is zero and equation (35) reduces to the standard definition for $R(\phi)$ in equation (2).

Transient batch settling tests may be used to determine $R(\phi)$, from very low solids concentrations up to solids concentrations in excess of the gel point. A single settling experiment at a given ϕ_o will yield a single $R(\phi)$ data point. Hence, application of this approach requires measurement of the initial rate of settling of the sediment/supernatant interface in a number of settling cylinders with different initial

solids concentrations above or below the gel point. It is also important to note that the determination of $R(\phi)$ via this method for suspensions with $\phi_o > \phi_g$ requires a concurrent determination of $P_y(\phi)$ at similar solids concentrations.

The low $R(\phi)$ data shown previously in figure 4 (below 10^{11}) were determined using the transient batch settling method. It is notable that the values for $R(\phi)$ span up to 8 orders of magnitude, yet a strong, smooth functional form is indicated over that range. Based on the definition of $R(\phi)$, it is expected that in the limit of zero volume fraction, $R(\phi)$ should reduce to λ/V_p. Thus in theory, to obtain a realistic functional form for $R(\phi)$, this behaviour should be implicit in the functional form used. By plotting $R(\phi)$ data versus $log\ \phi$ it would be expected that an asymptote be observed at low ϕ or at least a turning point in the second derivative of the $R(\phi)$ versus ϕ data. Revisiting figure 4, where the $R(\phi)$ data for zirconia were plotted in this fashion, it is clear that at, or just below, the gel point for this suspension a clear change in the curvature of the data is observed, providing vindication of both the gel point determined and the testing method.

The transient settling approach for characterisation of the permeability / hindered settling quantity has also been used by other researchers. Shirato et al. [74] used a similar approach to determine the specific cake resistance but compressive effects were not considered quantitatively. Auzerais et al. [82] and Eckert et al. [12] utilised the same basic equation presented in equation (35) for the analysis of transient data obtained from sedimentation in a centrifugal field.

Hindered Settling Function / Network Permeability - Permeation Testing

The simplest test procedure for the determination of the permeability of a network is through the constant pressure permeation of liquid through a packed bed of known height and concentration [30]. From Darcy's law, with a pressure drop ΔP across a packed bed of height, H, solids volume fraction, ϕ and with a liquid viscosity, η and neglecting membrane resistance, the volumetric flow-rate of liquid per unit area of membrane, dV/dt is given by:

$$\frac{dV}{dt} = \frac{\Delta P}{\eta\left(\dfrac{H}{k(\phi)}\right)} \qquad \qquad \dots\dots\dots(36)$$

Therefore, using equation (15) :

$$R(\phi) = \left(\frac{\Delta P}{dV/dt}\right)\frac{1}{H}\frac{1-\phi}{\phi} \qquad \qquad \dots\dots\dots(37)$$

Thus, by setting up a bed of known solids concentration, ϕ, and known bed thickness, H, $R(\phi)$ may be measured by applying a constant known head of fluid across the bed and measuring the rate of liquid flow.

Traditionally this type of test is conducted on relatively concentrated beds or pre-formed cakes or compacts. This approach forms the basis of the standard C-P test cell where a sample is filtered to equilibrium at a given pressure by a piston with a

porous end, as in a standard filtration test to give $P_y(\phi)$. Once the cake is formed, liquid is forced through the compact bed via the porous piston and the volumetric flow rate measured for a given pressure, allowing determination of the permeability. The applied pressure on the piston can then be increased, causing further consolidation of the cake allowing subsequent determination of the permeability at the new solids concentration. Applications of this approach are plentiful in the literature [eg. 88, 90].

Recent work indicates that the same test is possible on a much more dilute material at a solids concentration closer to the gel point. This involves allowing a suspension to settle to a loose sediment under gravity within a cylinder with a membrane at its base. By then maintaining a constant head of liquid above this bed, constant pressure permeation occurs. In practice the action of the permeating liquid causes some consolidation of the solids in the bed during the experiment, but the bed height eventually stabilises allowing a stable set of dV/dt, H and ϕ data to be obtained. Thus, $R(\phi)$ may be determined from equation (37) for the average solids concentration in the stabilised bed.

A single $R(\phi)$ data point obtained using gravity permeation is presented in figure 4 for a zirconia suspension which shows reasonable agreement with other methods. There are inherent limitations with quoting an average $R(\phi)$ for an average solids, where in reality for sediments of lower compressive strength a solids concentration distribution exists. However, working with higher solids suspensions results in other problems associated with entrapment of air bubbles in the sample on loading. Landman and White [2] proposed a more rigorous approach to utilising this type of test for the determination of $R(\phi)$ but application of the proposed approach by Green [57] met with limited success.

Hindered Settling Function / Network Permeability - Filtration Testing

A standard constant pressure filtration test may also be employed to determine $R(\phi)$ at higher solids concentrations. The use of the slope of a plot of T/V versus V (or T versus V^2) data from a constant pressure filtration, where T is the filtration time and V is the volume of filtrate per unit area of filter, for the determination of α is well known [23, 31]. A typical single pressure filtration test result is presented in figure 7 for a zirconia suspension [7]. The specific cake resistance may be determined from (or a similar equation, depending on the physical quantities used and measured):

$$ t = \frac{\eta \alpha \phi_o}{2 \Delta P (\phi - \phi_o)} V^2 + \frac{\eta R_m}{\Delta P} V \qquad\qquad \text{..........(38)} $$

where ϕ is the average solids concentration in the forming filter cake, which can be estimated either from direct measurement or graphically from the filtration test data at the end of the cake formation phase of filtration and the onset of cake compression [68]. The second term of the equation accounts for the resistance of the membrane, which in many cases is neglected. By performing constant pressure tests at a range of pressures, the permeability versus solids behaviour may be determined.

A well acknowledged limitation of this approach is the fact that the value of α determined is only an average value, given that the solids concentration distribution
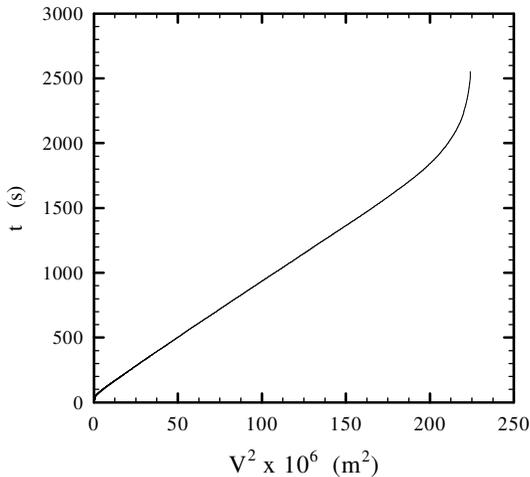
Figure 7: Filtration plot for 50 kPa constant, single pressure filtration of 10% v/v zirconia suspension. (zirconia, pH 6.8, 0.01M KNO$_3$, h_o = 0.02287 m) (adapted from de Kretser et al. [7])

within the forming cake for all but totally incompressible materials is non-constant [eg. 24, 26, 91]. In spite of this, aside from the more correct C-P cell approach to determining permeability, this is still the most widely accepted method of determining the permeability of high concentration cakes and remarkably good filtration data have been obtained that adhere to this semi-empirical model [68].

Landman, et al. [15] demonstrated however, that the same *T/V* versus *V* behaviour can be predicted from the full consolidation theoretical approach but from a different basis and with different assumptions. They also demonstrated that the same slope of the *T/V* versus *V* (or *T* versus *V^2*) plots, denoted β^2 in their work, could be used for the determination of *R(ϕ)* [67,18]. The difference is that the approach proposed determines a local volume fraction dependent measure of the permeability, rather than an average value as in equation (38). The following equation is used to determine *R(ϕ)* from, β^2, as a function of applied pressure, *ΔP*:

$$R(\phi_\infty) \equiv \left(\frac{\lambda}{V_p} \right) r(\phi_\infty) = \frac{2}{\dfrac{d\beta^2}{d\Delta P}} \left(\frac{1}{\phi_o} - \frac{1}{\phi_\infty} \right) (1 - \phi_\infty)^2$$

.........(39)

where ϕ_∞ is the equilibrium volume fraction at *ΔP*, and ϕ_o is the initial solids concentration of the filtration. Thus multiple filtration tests are required at a range of pressures and to calculate the derivative, *$d\beta^2/d\Delta P$*, the β^2 versus *ΔP* data are usually

plotted and fitted with a power law and the derivative of the fitting equation used in the calculation of $R(\phi)$.

Using the standard single, constant pressure filtration approach, each filtration test would be conducted at a different pressure, yielding a $P_y(\phi)$ data point and a β^2 versus ΔP data point. Calculation of $R(\phi)$ requires data at number of different pressures. Recently, as with the determination of $P_y(\phi)$, a technique of applying consecutive pressure steps to the same sample has been developed and refined to the point where a single filtration run allows determination of β^2 for all desired pressures in rapid time over a pressure range from 1 up to 400 kPa [7]. The only limitation of this stepped pressure permeability test is that all pressures are tested and β^2 determined prior to the end of the cake formation stage in the filtration test (as indicated by onset of the exponentially decaying phase of the filtration plot in figure 7).

In tandem with the stepped pressure compressibility test to determine ϕ_∞ data as a function of pressure, $R(\phi)$ may then be determined via equation (39) as before. The advantage of the stepped pressure filtration approach is the characterisation of $P_y(\phi)$ and $R(\phi)$ for a sample over many pressures in only two filtration tests. Data for $R(\phi)$ determined via this method is presented in figure 4 and agrees well with $R(\phi)$ data determined via other methods. Validation of the stepped pressure approach has been provided both through comparison of single pressure filtration test data with stepped pressure data [7], Darcian modelling of the behaviour of the filter cake on stepping of the pressure [8] and comparison of real transient stepped pressure filtration test data with predictions based on $P_y(\phi)$ and $R(\phi)$ data used in an analytical filtration model [16] adapted for stepped pressure conditions [19].

3. APPLICATIONS OF THE DE-WATERING FRAMEWORK

Over the past 15 years, mathematical models based on fundamental force balances have been developed for the modelling of most common de-watering devices such as filters [16], thickeners [4, 36] centrifuges [1, 12, 37] and the simple tailings pond [9, 34]. The de-watering parameters discussed in this review form the material parameter inputs for all of these theoretical de-watering frameworks. Thus, the capacity exists to view the effects of chemical additives such as polymeric flocculants on the de-waterability of mineral suspensions and optimise their addition. A significant issue with the addition of flocculants is the shear conditions in which flocculation is conducted – for the same polymer added at the same dose in different shear conditions, the flocs produced can differ in size and structure. Being able to quantify the de-waterability of materials produced under varying conditions allows optimisation of floc structure for de-watering.

Obviously, once conditions for de-watering have been optimised, the shear rheology of the materials produced must be evaluated and taken into account. Thus, an overall picture of what is required, rheologically, to optimise the processing of a solid-liquid system can be developed.

Numerous studies of the effect of surface chemical behaviour and physical properties on the compressive and permeability behaviour of solid-liquid systems have been undertaken. Early work by Callaghan and Ottewill [86] used compression cell

measurements on clay to correlate with the interparticle forces in the system. Grace [88] and Wakeman et al. [68] both investigated the effect of particle size and level of flocculation on filter cake compressibility and permeability. A number of studies on model systems have investigated the effect of interparticle force on $P_y(\phi)$ and $R(\phi)$ such as latex [39], alumina [83, 58, 42] and zirconia [41, 67] . Work by Zhou et al. [43] focussed on the effect of particle size on $P_y(\phi)$ for alumina suspensions and the alumina system was also the subject of a study of the effects of microstructure on $P_y(\phi)$ (92). Recent work has focussed on quantifying the effect of polymeric flocculation on de-waterability [93].

In spite of the utility of properly measured compressibility and permeability techniques for optimising and understanding compressive de-watering, in many cases, because of the integral nature of the solutions of the non-linear differential equations, the only way to conclusively evaluate and compare the effect of different parameters on the performance of an engineering solid liquid separation operation is to evaluate the full model predictions for each case. Furthermore, a simple, yet important observation is that in most cases industrial operations which are focussed on increased throughput operate at solids fluxes such that the output solids is far from the equilibrium solids characteristic of the applied de-watering pressure. As such, optimisation of the de-watering process will be dominated by optimising $R(\phi)$ rather than $P_y(\phi)$. In the next sections, in addition to briefly reviewing the main modelling approaches taken for filtration, sedimentation and continuous thickening, a demonstration of the effect of variations in $P_y(\phi)$ and $R(\phi)$ on the predicted unit operation performance will be presented.

Figures 8 and 9 present curve fits for $P_y(\phi)$ and $R(\phi)^{-1}$ (permeability) data (taken from [94]) generated from fitting of results for calcite suspensions flocculated at constant dose of polymeric flocculant, but under varied shear conditions. It can be seen that there are significant differences in both compressibility and permeability as a result of changing the nature of the floc structure formed during flocculation. Each of the $P_y(\phi)$ and $R(\phi)$ plots show a high and low compressibility and permeability respectively. In subsequent sections in this review simulations of filtration and thickening will be presented, based on input to the models of combinations of low-low, low-high, high-low and high-high compressibility-permeability data based on the results in figures 8 and 9.

Filtration

There has been a huge amount of work conducted in the area of filtration modelling using full numerical, spatial coordinate approaches, both from within the Landman-White approach [13, 14, 49, 15, 37] and the more traditional Tiller-Shirato school of filtration work [24, 95, 26, 96, 25]. Material coordinate approaches have also been undertaken by a number of workers [eg 97, 17, 84, 87, 98, 18]. Extension of the full numerical theories to include the incidence of sedimentation during the course of filtration has also been completed with favourable comparison to experimentally determined results [14, 49]. Tiller et al. [99] used a modified version of the simpler average specific cake resistance approach for the modelling of filtration with sedimentation with reasonable prediction of the main experimental features observed.
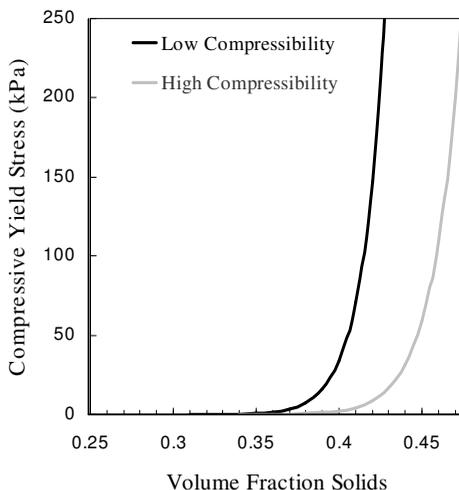
Figure 8: Synthetic $P_y(\phi)$ data derived from real data for polymer-flocculated calcite suspensions (adapted from de Kretser et al.[94].
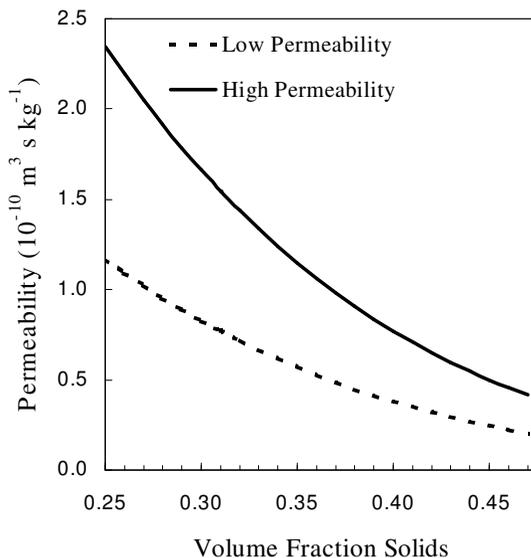

Figure 9: Synthetic permeability $(R(\phi)^{-1})$ data derived from polymer-flocculated calcite data (adapted from de Kretser et al. [94]).

Most of these models a have been shown to predict the behaviour of real filtration systems with reasonable accuracy for a wide range of materials and the authors of each theory claim it has advantages over the other either in terms of its ease of use or accuracy.

In practice the basic modelling approaches used in each case are similar, a fact that has been noted in some works [100, 69] and the variability in model predictions associated with the constitutive models used in the theories is possibly as great as the differences between the model predictions themselves. Hence benchmarking and sensitivity analyses of the different approaches should be performed.

Another significant limitation of most numerical approaches is their lack of ease of use as an engineering tool. Landman and White [16] approached this problem via the linearisation of the filtration theory using first a coordinate change to material coordinates and then use of a linearisation approximation. The linearised filtration theory still predicts classic "two-stage" behaviour of filtration with cake formation followed by cake compression. The theory predicts linear t vs. V^2 behaviour in the cake formation region in accordance with the following equation (derived from equation (B9) in [16]) where t is the filtration time and V is the specific volume of filtrate:

$$ t = h_0^{\,2} \left(\frac{\phi_0}{\phi_\infty} \right)^2 \frac{T_c}{D_\infty (h_0 - h_c)} V^2 \qquad\qquad\ldots\ldots\ldots(40) $$

where ϕ_O and ϕ_∞ are the initial and final solids concentrations and h_0 is the initial height of material in the filter. T_c is the dimensionless time at which the cake formation period ends and cake compression commences and h_c is the piston height at which this occurs. D_∞ is the diffusivity at the final solids concentration (ϕ_∞). Thus, as all of the terms grouped in front of the V^2 are constant for a given applied pressure, linear behaviour in t versus V^2 is predicted.

The solution of the equations to obtain an explicit time-volume relationship for the cake compression region required an approximation involving truncation of a Fourier series. The resulting equation, derived from equation (113) in [16], exhibits a logarithmic functional form for the cake compression region and may be simplified to:

$$ t = E_1 - E_2 \ln(E_3 - V) \qquad\qquad\ldots\ldots\ldots(41) $$

where E_1 is a constant depending on the diffusivity behaviour as a function of volume fraction, the initial and final volume fraction solids, the initial height of suspension and the first term in the Fourier series expansion,

$$ E_2 = \frac{4h_0^2}{\pi^2 D_\infty} \left(\frac{\phi_0}{\phi_\infty} \right)^2 \qquad\qquad\ldots\ldots\ldots(42) $$

and:

$$E_3 = h_0\left(1 - \frac{\phi_0}{\phi_\infty}\right) \qquad\qquad \text{.........(43)}$$

Equation (41) predicts that within the cake compression region of filtration, a plot of t versus $ln\,(E_3 - V)$ will be linear assuming that ϕ_0, ϕ_∞ and h_0 are known.

Landman and White [16] did not validate their approach with experimental data, however a number of studies have been completed recently showing that use of the analytical solution predicts full single pressure filtration (both cake formation and cake compression behaviour) well [7]. Furthermore, the model was also adapted to model stepped pressure filtration and the model predictions compared to real data [19]. The results are shown in figure 10 and the agreement is exceptional over pressures from 1 to 300 kPa.

Use of the compressibility and permeability data from figures 8 and 9 in the Landman-White [16] model yielded the results presented in figure 11 for the operation of a constant pressure batch filter at 100 kPa with an initial feed suspension height of 1 m (somewhat unrealistic, but acceptable for the purpose of this comparison) at 0.25 volume fraction solids.

Clearly, for each of the suspensions that had a common compressibility, the final solids are the same, whilst the different permeabilities lead to varying filtration
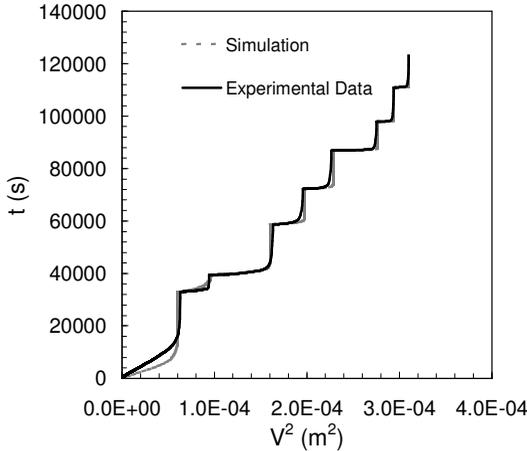
Figure 10: Comparison of simulation and experimental data for a multiple pressure compressibility test. (Zirconia, pH 7.0, $\phi_0 = 0.0809$, $h_0 = 0.02285$ m - adapted from de Kretser et al. [19]).
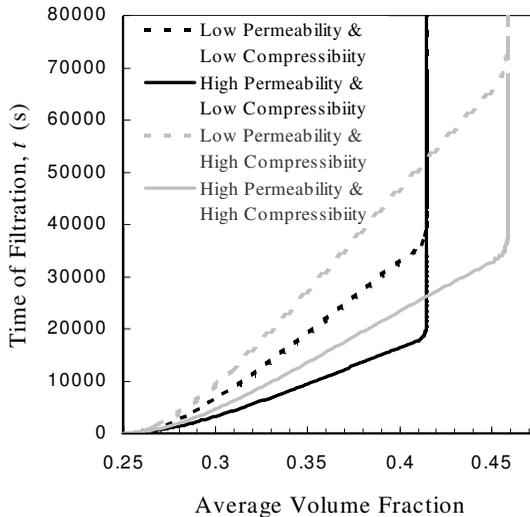
Figure 11: Filtration simulations for a batch filter press using calcite de-waterability data - P =100 kPa, ϕ_0 = 0.25, h_0 = 1 m. (adapted from de Kretser et al. [94])

times. The conclusion that the process is permeability dominated is clear from the longer filtration times for the low permeability samples. The optimum condition for minimising filtration cycle times depends on the desired average cake solids required from the filter. For ϕ_{av} > 0.41, the high compressibility, high permeability material is the only option, whilst for ϕ_{av} < 0.41, the optimum material to filter is the low compressibility-high permeability material.

The simple example presented in the preceding paragraph illustrates the types of application of the completed consolidation framework once $Py(\phi)$ and $R(\phi)$ data are available. Such an approach can potentially help operations in practice optimise pressures of operation, filter cycle times, chemical conditioning or investigate the effect of feed solids variation on filter productivity.

Sedimentation

The relative ease with which experimental data can be gathered for sedimentation processes is perhaps one reason why there is so much work in the literature dealing with modelling of batch sedimentation processes. Models for the behaviour of a batch settling process are numerous, yet, as is the case in filtration research, much of the theoretical work that treats the case of sedimentation of compressive sediments has a similar fundamental basis [eg. 79, 71, 1, 9, 101, 82, 34].

Many of these models are also easily extendable to modelling of sedimentation in a centrifugal field and in some cases this has been explicitly treated as a subject of study [102, 37].

It should be noted that the approach undertaken in the work of Howells et al. [9] for the solution of the sedimentation problem did not take into account the multiple solution conditions possible for the resolution of shocks within the compressible sediment. These phenomena were accounted for in other work by Auzerais et al. [82] and Garrido et al. [34] and can result in drastically different behaviour with respect to the solids concentration gradients within the sediment.

In most comparisons of theoretical predictions with experimental data for batch sedimentation, the agreement is generally good for well behaved systems both for predicting the rate of fall of the interface between the clear liquid and the top of the solids and also for the evolution of "characteristics" of constant concentration from the base of the settling vessel.

Thickening

The utilisation of compressive de-watering parameters for the modelling an industrial thickener is possible using existing theoretical frameworks. There are a number of equivalent 1-dimensional thickening theories currently employed in the literature based on the type of consolidation approach described in this review [9, 36]. Utilisation of the theoretical framework proposed by Landman et al. [4] for modelling of continuous thickening involves integration of a one dimensional differential equation relating the change in solids concentration with height in the thickener for a given solids flux and underflow solids concentration. The change in thickener cross sectional area with height in the thickener is accounted for through the use of a shape factor. which effectively makes the model 2-dimensional. The differential equation is iteratively solved (numerically) subject to the boundary conditions that the solids concentration is equal to the gel point at the top of the suspension bed and is equal to the given underflow solids concentration at the base of the thickener. Solution of the differential equation gives the underflow solids concentration, ϕ_u, for a given solids flux, q, and suspension bed height, h_b.

There are a number of significant assumptions used in the Landman et al. [4] model which limit its application – the model assumes steady state operation, no solids carryover in the overflow and that the effect of shear processes on de-watering in the thickener are negligible. Additionally, the Landman et al. [4] model suffers from the same limitations as the work of Howells et al. [9] with respect to the resolution of concentration shocks within the bed. The model inputs required are, aside from the $P_y(\phi)$ and $R(\phi)$ data over the range of solids concentrations of interest, the thickener dimensions, including diameter as a function of height, and the feed solids concentration. Note that the approach of Bürger has been adapted to incorporate transient effects [36].

Typical results presented in figure 12 show the relative performance of a thickener with a 5m bed height processing the calcite suspension described in figures 8 and 9 with the varying properties discussed previously. Results are presented as
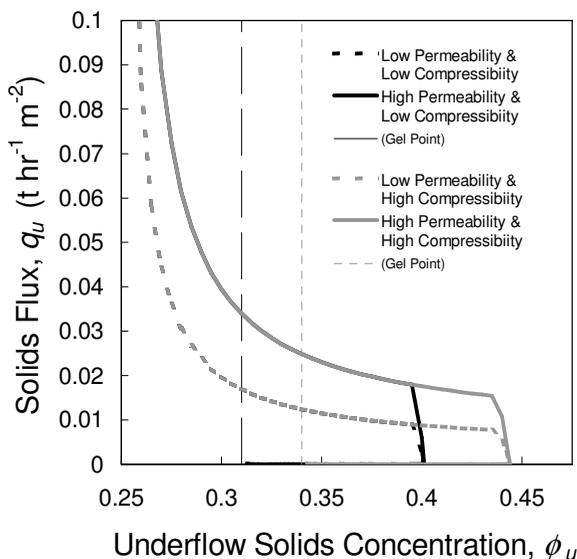
Figure 12: Steady state thickening simulations based on calcite de-waterability data for bed height = 5 m. (adapted from de Kretser et al.[94]).

underflow solids as a function of total solids flux. The results show that for very low fluxes, the underflow solids generated by the thickener is controlled by the compressibility of the materials processed. Under these operating conditions a dependency of the underflow solids on the bed height will be exhibited. However, as the solids flux is increased, the effect of permeability on the de-watering becomes increasingly important and a region exists at intermediate fluxes where the optimum underflow solids is dependent on both the compressibility and permeability. At higher solids fluxes again, the solids concentration in the underflow becomes dependent exclusively on the permeability or inter-phase drag of the solid liquid system. Under such operating conditions the model predicts very little or no dependence of the underflow solids on bed height (depending on whether the thickener is flat bottomed or not) indicating that the residence time of the material in the thickener is too short for appreciable compressive de-watering to occur.

Such analysis has significant implications on the way in which industrial thickeners are operated and the linking of this type of approach with characterisation of the effect of flocculation on de-waterability is becoming a useful tool in optimising plant operation. Early results indicate that, for systems in the absence of appreciable shear forces and raking, the model results compare very favourably with pilot scale thickening operation. Current work is progressing in investigating the effect of shear

on $P_y(\phi)$ and $R(\phi)$ to be able to model and exploit the anecdotally reported enhancement of shear on de-watering [103].

CONCLUSIONS

The area of compressive rheology, or compressive de-watering is expansive by virtue of its importance to a diverse range of industries including minerals processing, water and wastewater treatment and civil engineering and fundamental theories have correspondingly emerged from each of these areas. Given the amount of literature across these areas it has not been possible to review each in depth. In spite of this, this work has provided an overview of the main aspects of the theory and its limitations, how apparently different theories are interrelated, how modelling parameters are typically determined and how they can be applied in practical studies.

ACKNOWLEDGEMENTS

REFERENCES

1. Buscall R and White L R, J. Chem. Soc. Faraday Trans. I, 83 (1987) 873-891.

2. Landman K A and White L R, AIChE J, 38 (1992) 184-192.

3. Bergstrom L, Schilling C H and Aksay I A, Compressive Yield Stresses of Flocculated Particle Suspensions, In "Proc. XIth Int. Congr. Rheology", (Editors: Moldenaers P and Keunings R) Brussels, Elsevier (1992b) 579-581.

4. Landman K A, White L R and Buscall R, AIChE J, 34 (1988) 239-252.

5. Miller K T and Zukoski C F, J. Am Ceram. Soc., 77 (1994) 2473-2478.

6. Dixon D C, Separation Sci. Tech., 13 (1978) 753-766.

7. de Kretser R G, Usher S P, Scales P J, Landman K A and Boger D V, AIChE J, 47 (2001) 1758-1769.

8. Usher S P, de Kretser R G and Scales P J, AIChE J, 47 (2001) 1561-1570.

9. Howells I, Landman K A, Panjkov A, Sirakoff C and White L R, Applied Mathematical Modelling, 14 (1990) 77-86.

10. Buscall R, Colloids Surf., 5 (1982) 269-83.

11. Bergstrom L, Schilling C and Aksay I A, J. Am. Ceramic Soc., 75 (1992a) 3305-3314.

12. Eckert W F, Masliyah J H, Gray M R and Fedorak P M, AIChE J, 42 (1996) 960-972.

R. G. de Kretser, D. V. Boger and P. J. Scales, Rheology Reviews 2003, pp 125 -165.

13. Landman K A, Sirakoff C and White L R, Phys. Fluids A, 3 (1991) 1495-1509.

14. Landman K A and Russel W B, Phys. Fluids A, 5 (1993) 550-560.

15. Landman K A, White L R and Eberl M, AIChE J, 41 (1995) 1687-1699.

16. Landman K A and White L R, AIChE J, 43 (1997) 3147-3160.

17. Kirby J H and Smiles D E, Aust. J. Soil Res., 26 (1988) 561.

18. Landman K A, Stankovitch J M and White L R, AIChE J, 45 (1999) 1875-1882.

19. de Kretser R G, Scales P J and Usher S P, Practically Applicable Modelling of Cake Filtration, In "AFS Annual Meeting: Science and Technology of Filtration and Separations for the 21st Century", (Editors: Chiang S H and Lee S E) Tampa, Fl, USA, Advance in Filtration and Separation Technology, 17, American Filtration and Separations Society (2001) 23.

20. Terzaghi K and Peck P B, "Soil Mechanics in Engineering Practice", John Wiley, New York, (1948).

21. Gibson R E, England G L and Hussey M J L, Geotechnique, 17 (1967) 261-273.

22. Stickland A, Scales P and Styles J R, Geotechnical Testing Journal, submitted (2002).

23. Tiller F M, Chem. Eng. Prog., 51 (1955) 282-290.

24. Tiller F M and Shirato M, AIChE J, 10 (1964) 61-67.

25. Lee D J, Ju S P, Kwon J H and Tiller F M, AIChE J, 46 (2000) 110-118.

26. Tiller F M and Yeh C S, AIChE J, 33 (1987) 1241-1257.

27. Ruth B F, Montillon G H and Montonna R E, Ind. Eng. Chem ., 25 (1933) 153-161.

28. Tiller F M, Yeh C S, Tsai C D and Chen W, Filtration and Separation, 24 (1987) 121-126.

29. Tiller F M and Hsyung N B, Water Sci. Tech., 28 (1993) 1-9.

30. Ward A S, in "Filtration - Principles and Practices", M. J. Matteson and C. E. Orr, Marcel Dekker, NY (1987).

31. Wakeman R J and Tarleton E S, "Filtration: Equipment Selection, Modelling and Process Simulation", Elsevier Advanced Technology, UK, (1999).

32. Shirato M, Murase T, Negawa M and Fukaya S, J Chem Eng Japan, 4 (1971) 263-268.

33. Shirato M, Murase T, Tokunaga A and Yamada O, J Chem Eng Japan, 7 (1974) 229-231.

34. Garrido P, Bürger R and Concha F, Int. J. Mineral Process., 60 (2000) 213-227.

35. Bürger R, Concha F and Tiller F M, Chem. Eng. J., 80 (2000) 105-217.

R. G. de Kretser, D. V. Boger and P. J. Scales, Rheology Reviews 2003, pp 125 -165.

36. Bürger R, Bustos M C and Concha F, Int. J. Mineral Process., 55 (1999) 267-282.

37. Bürger R, Concha F and Karlsen K H, Chem. Eng. Sci., 56 (2001) 4537-4553.

38. Buscall R, McGowan I J, Mills P D A, Stewart R F, Sutton D, White L R and Yates G E, J. Non-Newtonian Fluid Mech., 24 (1987) 183-202.

39. Buscall R, Mills P D A, Goodwin J A and Lawson D W, J. Chem. Soc. Faraday Trans., 84 (1988) 4249-4260.

40. Meeten G H, Colloids Surfaces A: Physiochem. Eng. Aspects, 82 (1994) 77-83.

41. Green M D and Boger D V, Ind. Eng. Chem. Research, 36 (1997) 4984-4992.

42. Channell G M and Zukoski C F, AIChE J, 43 (1997) 1700-1708.

43. Zhou Z, Scales P J and Boger D V, Chem. Eng. Sci., 56 (2001) 2901-2920.

44. Barnes H A and Walters K, Rheol. Acta, 24 (1985) 323-326.

45. Hartnett J P and Hu R Y Z, J. Rheol., 33 (1989) 671-679.

46. Schurz J, Rheol. Acta, 29 (1990) 170-171.

47. Schurz J, J. Rheol., 36 (1992) 1419-1421.

48. Chang C, Boger D V and Nguyen Q D, Indust. Eng. Chem. Res., 37 (1998) 1551-1559.

49. Shen C, Russel W B and Auzerais F M, AIChE J., 40 (1994) 1876-1891.

50. Zhou Z, "Rheology of Metal Oxide Suspensions", Ph D Thesis, University of Melbourne, (2000).

51. Leong Y K, Scales P J, Healy T W and Boger D V, J. Am. Ceram. Soc., 78 (1995) 2209-2212.

52. Johnson S B, Russell A S and Scales P J, Colloids and Surfaces A: Physicochemical and Engineering Aspects , 141 (1998) 119-130.

53. Leong Y K, Boger D V, Scales P J, Healy T W and Buscall R, J. Chem. Soc., Chemical Communications (1993) 639-641.

54. Liddell PV, "The Rheology of Titanium Dioxide Pigment Suspensions", PhD Thesis, University of Melbourne, (1996).

55. Kapur P C, Scales P J, Boger D V and Healy T W, AIChE J, 43 (1997) 1171-1179.

56. Scales P J, Kapur P C, Johnson S B and Healy T W, AIChE J, 44 (1998) 538-544.

57. Green M D, "Characterisation of Suspensions in Settling and Compression", PhD Thesis, University of Melbourne, University of Melbourne, (1997).

58. Miller K T, Melant R M and Zukoski C F, J. Am Ceram. Soc., 79 (1996) 2545-2556.

R. G. de Kretser, D. V. Boger and P. J. Scales, Rheology Reviews 2003, pp 125 -165.

59.   Shin B S and Dick R J, Prog. Water Technology, 7 (1975) 137-147.

60.   Nguyen Q D and Boger D V, J. Rheol., 29 (1985) 335-347.

61.   Chen L B and Zukoski C F, J. Chem. Soc. Faraday Trans., 86 (1990) 2629-2639.

62.   Uriev N B and Ladyzhinsky I Ya, Colloids and Surfaces, 108 (1996) 1-11.

63.   Kapur P C, Colloids and Surfaces A: Physicochemical and Engineering Aspects, 146 (1999) 25-32.

64.   Bowen W R and Jenner F, Chem. Eng. Sci., 50 (1995) 1707-1736.

65.   Koenders M A and Wakeman R J, Chem. Eng. Sci., 51 (1996) 3897-3908.

66.   Green M D, Eberl M, Landman K L and White L R, AIChE J., 42 (1996) 2308-2318.

67.   Green M D, Landman K A, de Kretser R G and Boger D V, Ind. Eng. Chem. Research, 37 (1998) 4152-4156.

68.   Wakeman R J, Sabri M N and Tarleton E S, Powder Technology, 65 (1991) 283-292.

69.   Tien C, Powder Tech., in press (2002).

70.   de Kretser R G, Usher S P and Scales P J, J .Mineral Process., submitted (2002).

71.   Tiller F M and Khatib Z, J. Colloid Int. Sci. 100 (1984) 55-67.

72.   Chen M and Russel W B, Journal of Colloid and Interface Science, 141 (1991) 564-577.

73.   Rueb C J and Zukoski C F, J Rheol., 42 (1998) 1451-1476.

74.   Shirato M, Murase T, Iritani E and Hayashi N, Filtration and Separation, 20 (1983) 404-406.

75.   Buscall R, Stewart R F and Sutton D, Filt. Sep., 21 (1984) 183-188.

76.   De Guingand N J, "The Behaviour of Flocculated Suspensions in Compression", Masters Thesis, University of Melbourne, (1986).

77.   Miller KT et al. "Compressive Yield Stress of Cement Paste", in "Microstructure of Cement-Based Systems / Bonding and Interfaces in Cementitious Materials", Materials Research Society, (1995) 285-291.

78.   de Kretser R G, Scales P J and Boger D V, AIChEJ., 43 (1997) 1894-1903.

79.   Shirato M, Kato H, Kobayashi K and Sakazaki H, J. Chem. Eng. Japan, 3 (1970) 98-104.

80.   Holdich R G and Butt G, Minerals Engineering, 9 (1996) 115-131.

81.   Buscall R and Mc Gowan I J, J. Chem. Soc. Faraday Discuss., 76 (1983) 277-290.

R. G. de Kretser, D. V. Boger and P. J. Scales, Rheology Reviews 2003, pp 125 -165.

82.   Auzerais F M, Jackson R, Russel W B and Murphy W F, J Fluid Mech, 221 (1990) 613-639.

83.   Bergström L, J. Chem. Soc. Faraday Trans., 88 (1992) 3201-211.

84.   Sherwood J D, Meeten G H, Farrow C A and Alderman N J, J. Chem. Soc. Faraday Transactions, 87 (1991) 611-618.

85.   Meeten G H, Chem. Eng. Sci., 48 (1993) 2391-2398.

86.   Callaghan I C and Ottewill R H, J.Chem. Soc. Faraday Disc., 57 (1974) 110-118.

87.   Sherwood J D and Meeten G H, J. Petrol. Sci. & Eng., 18 (1997) 73-81.

88.   Grace H P, Chemical Engineering Progress, 47 (1953) 303-318.

89.   Lester D R, Usher S P, de Kretser R G and Scales P J, J. Mineral Process., submitted (2002).

90.   Teoh S K, Reginald B H, Tan B H and Tien C, Separation and Purification Technology, in press (2002).

91.   Tosun I, Yetis U, Willis M S and Chase G G, Water Science Technology, 28 (1993) 91-101.

92.   Channell G M, Miller K T and Zukoski C F, AIChE J., 46 (2000) 72-78.

93.   Aziz A A A, de Kretser R G, Dixon D R and Scales P J, Water Science and Technology, 41 (2000) 9-16.

94.   de Kretser R G, Scales P J, Boger D V and Usher S P, Compression De-watering of Suspensions: From Fundamentals to Application , In "Proc. XIIIth Int. Congr. Rheol.", (Editors: Binding D M, Hudson N E, Mewis J, Piau J-M, Petrie C J S, Wagner M H and Walters K) Cambridge, UK, British Soc. Rheol. Glasgow (2000) 29.

95.   Tiller F M, in "The Scientific Basis of Filtration",   (Editor: Ives K J), Noordhoff, Leyden (1975).

96.   Stamatakis K and Tien C, Chem. Eng. Sci., 46 (1991) 1917.

97.   Smiles D E, in "Encyclopedia of Fluid Mechanics", Vol. 5, (Editor: Cheremisinoff N P), Gulf Publishing (Houston, TX) (1986) Vol. 5.

98.   Sherwood J D, AIChE J, 43 (1997) 1488-1493.

99.   Tiller F M, Hsyung N B and Cong D Z, AIChE J, 41 (1995) 1153-1164.

100.   Tien C, Water Res. 35 (2001) 1367-1368.

101.   Auzerais F M, Jackson R and Russel W B, J. Fluid Mech., 195 (1988) 437-62.

102.   Sambuichi M, Nakakura H and Osasa K, J Chem. Eng. Japan, 24 (1991) 489-494.

103.   Johnson S B, Scales P J, Dixon D R and Pascoe M, Water Research, 34 (2000) 288-294.